

PAPER • OPEN ACCESS

The PAMELA experiment: a decade of Cosmic Ray Physics in space

To cite this article: A M Galper *et al* 2017 *J. Phys.: Conf. Ser.* **798** 012033

View the [article online](#) for updates and enhancements.

You may also like

- [Evidence of Energy and Charge Sign Dependence of the Recovery Time for the 2006 December Forbush Event Measured by the PAMELA Experiment](#)
R. Munini, M. Boezio, A. Bruno et al.
- [OBSERVATIONS OF THE 2006 DECEMBER 13 AND 14 SOLAR PARTICLE EVENTS IN THE 80 MeV \$n^{1-3}\$ GeV \$n^1\$ RANGE FROM SPACE WITH THE PAMELA DETECTOR](#)
O. Adriani, G. C. Barbarino, G. A. Bazilevskaya et al.
- [MEASUREMENTS OF COSMIC-RAY HYDROGEN AND HELIUM ISOTOPES WITH THE PAMELA EXPERIMENT](#)
O. Adriani, G. C. Barbarino, G. A. Bazilevskaya et al.



ECS
The
Electrochemical
Society
Advancing solid state &
electrochemical science & technology

DISCOVER
how sustainability
intersects with
electrochemistry & solid
state science research

The PAMELA experiment: a decade of Cosmic Ray Physics in space

A M Galper¹, R Sparvoli^{2,3}, O Adriani^{4,5}, G Barbarino^{6,7}, G A Bazilevskaya⁸, R Bellotti^{9,10}, M Boezio¹¹, E A Bogomolov¹², M Bongi^{4,5}, V Bonvicini¹¹, S Bottai⁵, A Bruno¹⁰, F Cafagna¹⁰, D Campana⁷, P Carlson¹³, M Casolino^{3,14}, G Castellini¹⁵, C De Donato³, C De Santis³, V Di Felice^{3,16}, A V Karelin¹, S V Koldashov¹, S A Koldobskiy¹, S Y Krutkov¹², A N Kvashnin⁸, A A Leonov¹, V V Malakhov¹, L Marcelli³, M Martucci^{2,3}, A G Mayorov¹, W Menn¹⁷, M Mergè^{2,3}, V V Mikhailov¹, E Mocchiutti¹¹, N Mori^{4,5}, R Munini¹¹, G Osteria⁷, F Palma^{2,3}, B Panico⁷, P Papini⁵, M Pearce¹³, P Picozza^{2,3}, M Ricci¹⁸, S B Ricciarini^{15,5}, M Simon¹⁸, P Spillantini^{4,5}, Y I Stozhkov⁸, A Vacchi¹⁹, E Vannuccini⁵, G I Vasilyev¹², S A Voronov¹, Y T Yurkin¹, G Zampa¹¹ and N Zampa¹¹

¹ National Research Nuclear University MEPhI, RU-115409, Moscow, Russia

² Department of Physics, University of Rome "Tor Vergata" I-00133 Rome, Italy

³ INFN, Sezione di Rome "Tor Vergata", I-00133 Rome, Italy

⁴ University of Florence, Department of Physics, I-50019 Sesto Fiorentino, Florence, Italy

⁵ INFN, Sezione di Florence, I-50019 Sesto Fiorentino, Florence, Italy

⁶ University of Naples "Federico II", Department of Physics, I-80126 Naples, Italy

⁷ INFN, Sezione di Naples, I-80126 Naples, Italy

⁸ Lebedev Physical Institute, RU-119991 Moscow, Russia

⁹ University of Bari, I-70126 Bari, Italy

¹⁰ INFN, Sezione di Bari, I-70126 Bari, Italy

¹¹ INFN, Sezione di Trieste, I-34149 Trieste, Italy

¹² Ioffe Physical Technical Institute, RU-194021 St. Petersburg, Russia

¹³ KTH, Department of Physics, and the Oskar Klein Centre for Cosmoparticle Physics, AlbaNova University Centre, SE-10691 Stockholm, Sweden

¹⁴ RIKEN, Advanced Science Institute, Wako-shi, Saitama, Japan

¹⁵ IFAC, I-50019 Sesto Fiorentino, Florence, Italy

¹⁶ Agenzia Spaziale Italiana (ASI) Science Data Center, I-00044 Frascati, Italy

¹⁷ Universitat Siegen, Department of Physics, D-57068 Siegen, Germany

¹⁸ INFN, Laboratori Nazionali di Frascati, Via Enrico Fermi 40, I-00044 Frascati, Italy

¹⁹ University of Trieste, Department of Physics, I-34147 Trieste, Italy

E-mail: amgalper@mephi.ru

Abstract. The PAMELA detector was launched on June 15th of 2006 on board the Russian Resurs-DK1 satellite and during ten years of continuous data-taking it has observed very interesting features in cosmic rays, especially in the fluxes of protons, helium and electrons. Moreover, PAMELA measurements of cosmic antiproton and positron fluxes and positron-to-all-electron ratio have set strong constraints to the nature of Dark Matter. Measurements of boron, carbon, lithium and beryllium (together with the isotopic fraction) have also shed new light on the elemental composition of the cosmic radiation. Search for signatures of more exotic processes (such as the ones involving Strange Quark Matter) has also been pursued.



Furthermore, over the years the instrument has allowed a constant monitoring of the solar activity and a prolonged study of the solar modulation, improving the comprehension of the heliosphere mechanisms. PAMELA has also measured the radiation environment around the Earth, and detected for the first time the presence of an antiproton radiation belt surrounding our planet. In this highlight paper PAMELA main results will be reviewed.

1. The PAMELA mission

The Payload for Antimatter-Matter Exploration and Light-nuclei Astrophysics PAMELA satellite experiment was designed to study the charged component of the cosmic radiation - focusing on antiparticles - and was launched with a Soyuz-U rocket on June 15th of 2006 from the Baikonur cosmodrome (Kazakhstan). The apparatus is hosted on the Russian Resurs-DK1 satellite; at first the orbit was elliptical (altitude varying between 355 and 584 km) and semipolar (inclination of about 70°) and with a period of about 94 minutes. In 2010 the orbit was set to be circular with an almost fixed altitude of about 550 km. The mission was planned to last 3 years, but it was prolonged until 2016.

The PAMELA main scientific objectives were to measure the antiproton spectrum up to 200 GeV, the positron spectrum up to 200 GeV, the electron spectrum up to 600 GeV, the proton and helium nuclei spectra up to 1.2 and 0.6 TeV/n respectively and the nuclei spectra (from Li to O) up to ~ 100 GeV/n but also to search for antinuclei (with a $\overline{\text{He}}/\text{He}$ sensitivity of 10^7), new forms of matter, e.g. strangelets and finally to detect possible structures in cosmic ray spectra from e.g. Dark Matter or new astrophysical sources. Furthermore PAMELA is well suited to conduct studies of cosmic-ray acceleration and propagation mechanisms in the Galaxy, solar modulation effects, the emissions of Solar Energetic Particles (SEPs) inside the heliosphere and investigate the particles in the Earth's magnetosphere.

2. The instrument

PAMELA detector was equipped with various instruments which guaranteed a great redundancy in case of unexpected malfunctioning of some sub-detectors and allowed to perform in-flight calibrations, evaluate efficiencies and provide different measurements of a single event. The detector is composed of the following systems:

- a Time-of-Flight (ToF) system, with segmented scintillator planes divided into 3 groups (S_1, S_2, S_3).
- a magnetic spectrometer to measure trajectories of the incoming particles
- an anticoincidence system with solid scintillators (CARD, CAT, CAS)
- an electromagnetic sampling calorimeter
- a shower tail-catcher scintillator
- a neutron detector

The core of the instrument is a Nd-Fe-B alloy permanent magnet (with residual magnetization of 1.3 T) with a microstrip silicon tracking system composed of 6 equidistant 300 μm thick planes that constitute a magnetic spectrometer used to determine the rigidity ($R = pc/Ze$) and the charge Z of particles crossing the cavity. The double-sided silicon sensors provide two independent impact coordinates on each plane and the blocks of the magnet are configured to provide an almost uniform magnetic field oriented along the y-direction inside a cavity ($13.1 \times 16.1 \text{ cm}^2$). The dimensions of the permanent magnet define the maximum geometrical factor of the PAMELA experiment to be $21.6 \text{ cm}^2 \text{ sr}$. A set of scintillators forms the anticoincidence system, which consists of 4 plastic scintillators (CAS) surrounding the sides of the magnet, one

covering the top (CAT) and a set of 4 plastic scintillators (CARD) that surrounds the volume between the first two Time-of-Flight planes. An electromagnetic imaging calorimeter, placed under the spectrometer, comprises 44 single-sided silicon sensor layers ($380\ \mu\text{m}$ thick) interleaved with 22 plates of tungsten absorber. It can distinguish between leptons and hadrons through the analysis of the shape of the shower they produce. It also measures the energy of electrons and positrons interacting in its volume and check the alignment of the tracker sensors. A Time-of-Flight system, composed of 6 layers of fast plastic scintillators segmented into orthogonal bars and arranged in 3 double planes (S_1 , S_2 and S_3) provides information on particle velocity β and trigger. Both ends of each scintillator bar are glued to a plastic light guide which is mechanically coupled to a photomultiplier. An additional plastic scintillator (S_4) is used to detect charged particles in case a shower is not completely contained in the calorimeter; it consists of a single square piece of 1 cm thick scintillator which is read out by 6 PMTs. Finally a neutron detector (36 proportional counters, filled with ^3He surrounded by a polyethylene moderator enveloped in a cadmium layer) at the bottom of the instrument complements the calorimeter in lepton-hadron discrimination. The entire apparatus is ~ 1.2 m high, has a mass of 470 kg and an average power consumption of 355 W. More details on the instrument can be found in [1].

3. Protons, helium nuclei and electron spectra

Hydrogen and helium are the most abundant components of galactic cosmic rays, constituting about 98% of the total flux and they are believed to be of primary origin. The energy spectra of hydrogen and helium have been measured by many experiments over the years. The first high-statistics and high-precision measurements, carried on by PAMELA from July 2006 to March 2008, are shown in figure 1(a) together with results of other experiments [2, 1]. Interesting spectral features were found in the data, with significant implications for the understanding of high-energy galactic processes. The PAMELA data presented in figure 1(a) reveal a hardening in the spectrum of both H and He. These results are in good agreement with previous results below 100 GeV/n and consistent with the spectral features of the measurements by ATIC-2 and CREAM [1] at higher energies. Below 10 GeV/n discrepancies are evident, but this can be ascribed to different epochs of solar activity. Both spectra show deviations from a single power law model, exhibiting a spectral hardening at a rigidity of about 230-240 GV. By means of a statistical analysis of the spectra, two main structures were recognized:

- Both the H and He spectra gradually soften in the rigidity range 30-230 GV.
- The spectra exhibit a spectral hardening at 232^{+35}_{-30} GV for H and 243^{+27}_{-31} GV for He.

The spectral changes could be a result of the diffusion of cosmic rays on a background plasma waves partially due to self-generation and partly due to externally generated turbulence from large spatial scales to smaller scales where cosmic rays can resonate. Details can be found in [2].

Moreover, precision measurements of the electron component in the cosmic radiation provide important information about the origin and propagation of cosmic rays in the Galaxy. PAMELA published results regarding negatively charged electrons between 1 and 625 GeV; this is the first time that cosmic-ray e^- have been identified above 50 GeV. Figure 1(b) shows the electron flux up to 625 GeV. The data shows that the electron spectrum can be described with a single power-law energy dependence with spectral index -3.18 ± 0.05 above the energy region influenced by the solar wind (>30 GeV). No significant spectral features are observed and the data can be interpreted in terms of conventional diffusive propagation models. Details can be found in [3]

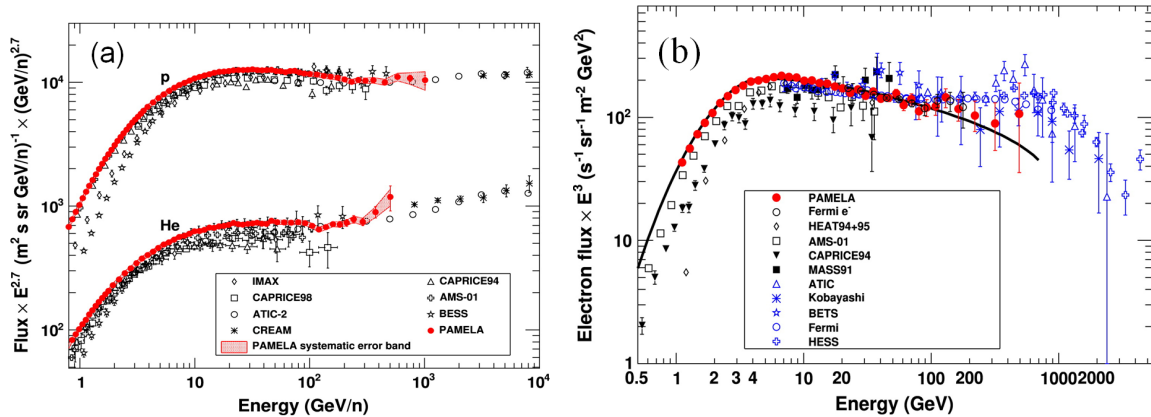


Figure 1. Proton and helium data (a) measured by PAMELA in the energy range from 1 GeV to ~ 1 TeV. Electron data (b) up to 625 GeV.

4. Boron and carbon nuclei

PAMELA has measured the absolute fluxes of boron and carbon and the B/C ratio, which plays a central role in galactic propagation studies in order to derive the injection spectra at sources from measurements at Earth [4]. During the propagation in the interstellar medium (ISM) from the acceleration sites to Earth, galactic cosmic rays undergo various physical processes which shape the injection spectra and chemical compositions down to the measured ones at Earth. The spectra of particles which are produced exclusively by interactions of primary particles with ISM provide good constraints to propagation parameters. In particular, boron nuclei in cosmic rays are produced mainly by spallation of carbon with contributions from other elements. Thus, the boron-to-carbon ratio (B/C) has been extensively studied in order to tune propagation models. Spectra of boron and carbon are shown in figure 2(a), while the B/C ratio is shown in figure 2(b), in the kinetic energy range 0.44-129 GeV/n [4].

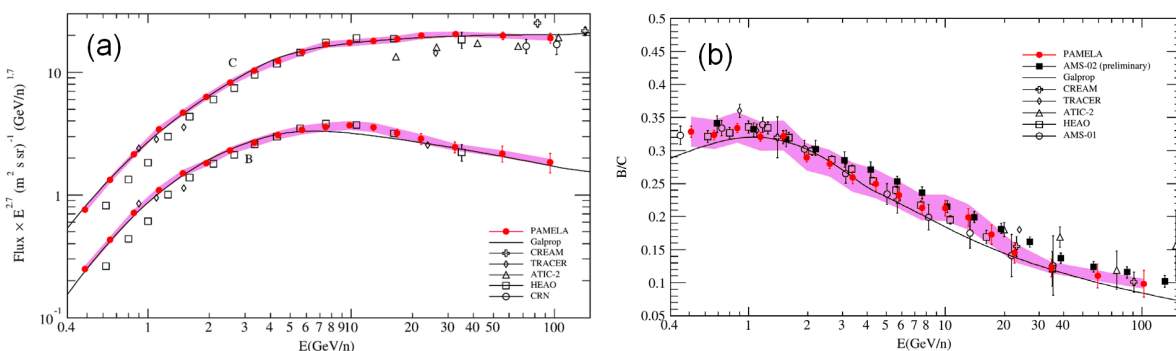


Figure 2. Boron and carbon fluxes multiplied by $E^{2.7}$ (a) and B/C flux ratio (b) as measured by PAMELA. Adapted from [4].

A good agreement with previous measurements can be observed, except at low energy where the effects of solar modulation are significant and must be carefully taken into account when comparing fluxes measured in different solar periods. The fitted spectral indexes above 20 GeV/n are 3.01 ± 0.13 for boron and 2.72 ± 0.06 for carbon. A very simple fit of PAMELA data based on

the GALPROP transport code gives a slope of the diffusion coefficient of 0.397 ± 0.007 , thus not allowing to discriminate between Kolmogorov and a Kraichnan diffusion types. However, this has been obtained with a specific transport model, and may vary when using different models.

5. Hydrogen, helium, lithium and beryllium isotopes

Measurements of the isotopic composition of elements of the cosmic radiation provide significant constraints on cosmic ray source composition and cosmic ray transport and acceleration in the Galaxy. For example, the rare isotopes ^2H and ^3He in cosmic rays are generally believed to be of secondary origin, resulting mainly from the nuclear interactions of primary cosmic-ray protons and ^4He with the interstellar medium. Moreover, while the ^6Li isotope is a pure product of interactions of galactic cosmic rays with this interstellar medium, the ^7Li isotope has several sources. In addition to the production of ^7Li by spallation during the propagation of cosmic rays, the stellar production and primordial nucleosynthesis of ^7Li are possible sources.

In PAMELA light nuclei, like lithium and beryllium, and rare isotopes are recognized by a full redundant set of dE/dx measurements provided by the apparatus (TOF, tracking-system and calorimeter), together with the velocity measurement by the Time-Of-Flight, to cleanly select these rare secondary elements against a large background of other particles.

PAMELA measurements for $^2\text{H}/^1\text{H}$, $^3\text{He}/^4\text{He}$, $^7\text{Li}/^6\text{Li}$ and $^7\text{Be}/(^9\text{Be} + ^{10}\text{Be})$ are shown respectively in figure 3(a), figure 3(b), figure 4(a) and figure 4(b).

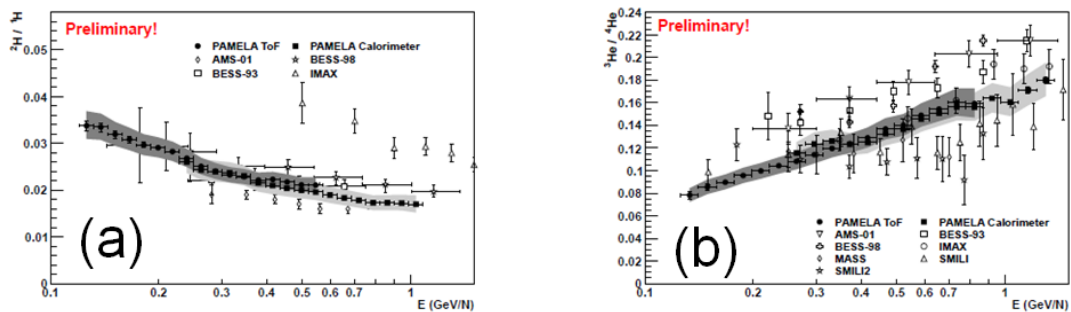


Figure 3. Results for the ratios $^2\text{H}/^1\text{H}$ (a) and $^3\text{He}/^4\text{He}$ (b) derived with the ToF or the calorimeter.

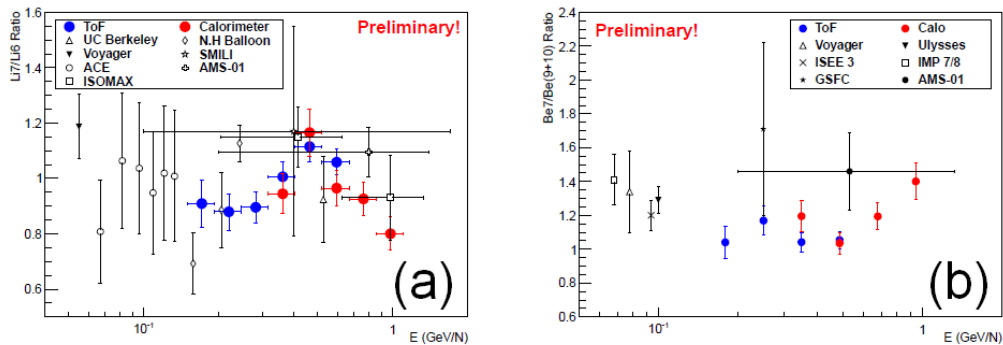


Figure 4. Results for the ratios $^7\text{Li}/^6\text{Li}$ (a) and $^7\text{Be}/(^9\text{Be} + ^{10}\text{Be})$ (b) derived with the ToF or the calorimeter.

It is visible that the PAMELA results in figure 3 are more precise in terms of statistics (this is due to the fact that other data, apart from the AMS-01 ones, are from balloon-borne experiments with limited data-taking and are effected by the non-negligible background of atmospheric secondary particle production). It is worth noticing that the PAMELA results obtained via the ToF analysis and via the multiple dE/dx measurements with the calorimeter agree very well within their systematic errors. This gives confidence to the results. Also for what concerns results for the ratios ${}^7\text{Li}/{}^6\text{Li}$ and ${}^7\text{Be}/({}^9\text{Be} + {}^{10}\text{Be})$, there is a good agreement between the ToF-derived measurements and the calorimeter-derived ones and with other experiments.

6. $\overline{\text{He}}/\text{He}$ and search for SQM

The explanation of the observed baryon asymmetry, i.e., the almost complete absence of antimatter in the visible part of the Universe, is one of the most important problems in cosmology. The real asymmetry value can be determined by direct measurements of the fluxes of antinuclei with charges $Z \geq 2$ in primary cosmic rays near the Earth. The results of the search for antihelium using data from the PAMELA experiment (June 2006 - December 2009) showed no events with $Z=2$ have been detected in the interval 0.6-600 GV. Thus, an upper limit on the $\overline{\text{He}}/\text{He}$ flux ratio has been set as a function of the energy and it is shown in figure 5(a). More details can be found in [5].

PAMELA presented also some results for direct search of Strange Quark Matter in cosmic rays [6]. If this state of matter exists, it may be present in cosmic rays as particles, called strangelets, having an anomalously high mass-to-charge (A/Z) ratio. A direct search in space is complementary in range and region to those coming from ground based spectrometers. In the energy range from 0.4 to ~ 1200 GV, corresponding to a mass range from 10 to ~ 105 a.m.u., no such particles were found in the data and thus an upper limit as a function of baryon number has been set and it is shown in figure 5(b) [6].

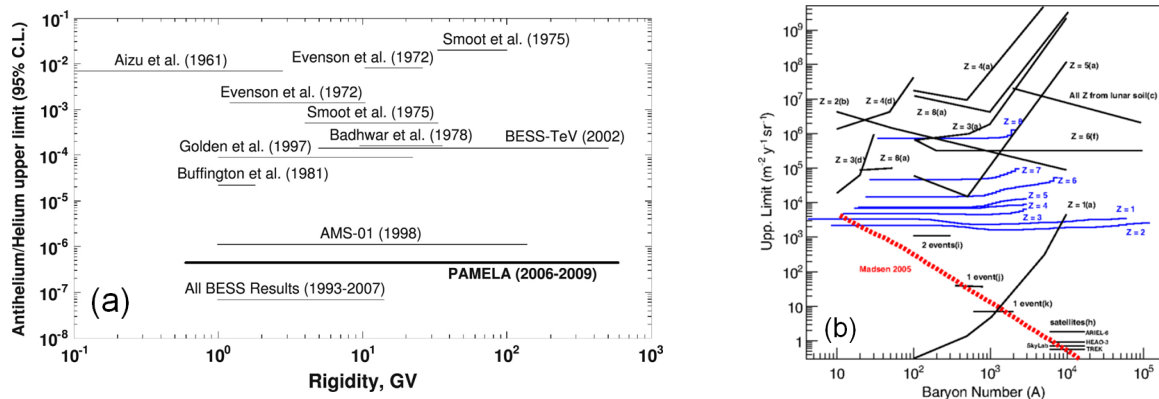


Figure 5. Upper limit on the $\overline{\text{He}}/\text{He}$ ratio (a), adapted from [5] and integral upper limits in terms of baryon number A as measured by PAMELA for $1 \leq Z \leq 8$ (b).

7. The antiparticle puzzle

Measurements of the presence of cosmic ray antiparticles (i.e. antiprotons and positrons), produced in the interaction between cosmic rays and the interstellar matter address many questions in contemporary astrophysics, such as the nature and distribution of particle sources in our Galaxy, and the subsequent propagation of the particles through the whole Galaxy and the solar magnetosphere. Moreover, new sources of primary cosmic ray antiparticles of either

astrophysical or exotic origin can be probed [1]. PAMELA measurements of antiproton-to-proton ratio, first published in [7] are shown in figure 6(a), while data of the $\frac{e^+}{e^++e^-}$ (first published in [8]) are shown in figure 6(b).

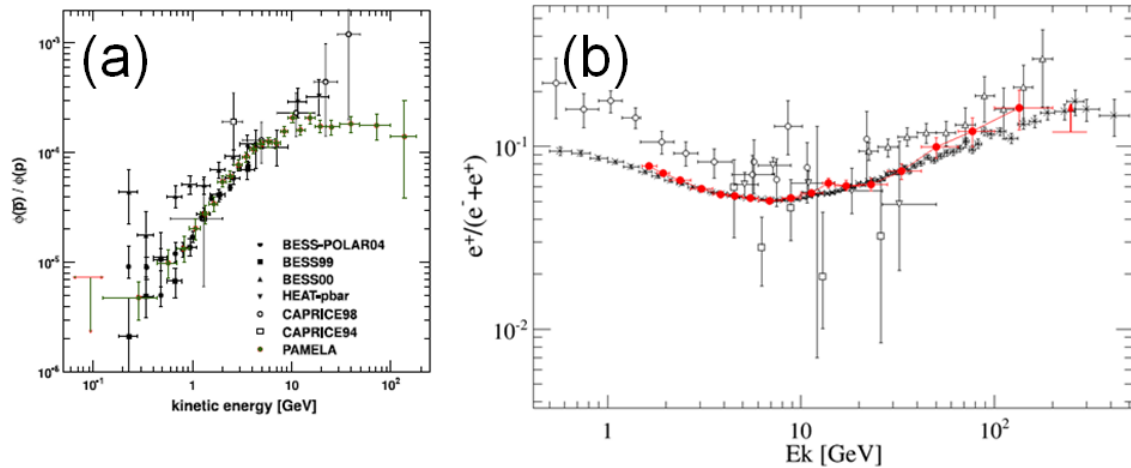


Figure 6. PAMELA results along with other recent measurements of the antiproton-to-proton flux ratio (a) and $\frac{e^+}{e^++e^-}$ (b). Adapted from [1].

PAMELA \bar{p} data (up to January 2010) are in good agreement, considering the uncertainties, with other data and they can be used to significantly constrain models of galactic Dark Matter such as those predicting heavy Weakly Interacting Massive Particle candidates. Also the low energy data are important because they can be used to constrain models with light (~ 10 GeV) Dark Matter candidates.

The resulting positron fraction measured by PAMELA between 1.5 and 300 GeV along with results from other recent experimental cosmic-ray space and balloon-borne experiments is shown in figure 6(b). Two features are clearly visible in the data:

- Below 5 GeV PAMELA results are systematically lower than other data.
- Above 10 GeV they show that the positron fraction increases significantly with energy, opposite to the expectation for secondary production.

The low energy discrepancy with data collected during the 1990s, i.e. from the previous solar cycle that favoured positively-charged particles, are interpreted as a consequence of solar modulation effects. At higher energies the agreement gives good confidence that the increase of the positron flux can be ascribed to a physical effect and not to systematic ones affecting the measurements. The high energy increase (that deviates from models has led to many speculations about a primary origin for the positrons. An excess in the positron population at high energy was postulated for the annihilation of Dark Matter particles in the galactic halo. While extremely intriguing, such an explanation is challenged by the asymmetry between the leptonic (positrons) and hadronic (antiprotons) PAMELA data. Such an asymmetry is difficult to explain in a framework where the neutralino is the dominant dark matter component. More detail can be found in [7, 3, 1].

8. Time dependence of proton, positron and electrons fluxes

The energy spectra of galactic cosmic rays, when measured near Earth, are significantly affected by solar wind and magnetic field. A comprehensive description of the cosmic radiation must

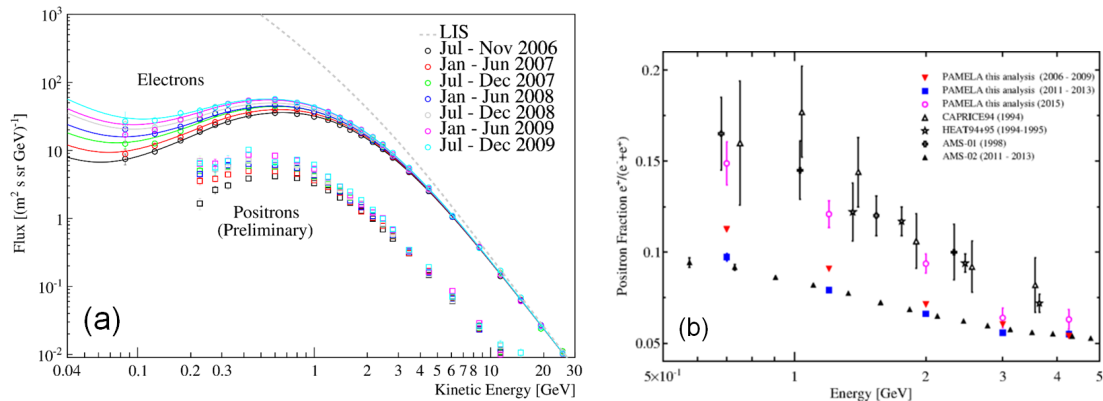


Figure 7. Time evolution of electron and positron fluxes (a) in the period 2006-2009 and time evolution of the e^+/e^- fraction during solar minimum, maximum and after the inversion of the solar magnetic polarity (b). For more details see [11].

therefore include the transport and modulation of cosmic rays inside the heliosphere. During the end of the last decade, the Sun underwent a peculiarly long quiet phase well suited to study modulation processes. PAMELA near-monthly (2006-2009) results on protons from 400 MV, compared with a state-of-the-art three-dimensional model of solar modulation, are presented in [9]. Other than protons, PAMELA observed the charge-sign dependent solar modulation effects also on electrons [10] and positrons [11]: the time variation of e^- , e^+ , and e^+/e^- fraction is presented in figure 7.

9. Solar Particle Events

The problem concerning the mechanism and site of Solar Energetic Particles (SEPs) acceleration remains an open question. SEPs may be produced after powerful explosive events on the Sun, accompanied by solar flares, coronal mass ejections, bursts of X/γ -rays and radio emission; it is clear that not a single mechanism is not involved in their formation. PAMELA started to observe SEPs fluxes during the 2006, December 13th/14th events which also represent the first direct measurement of SEPs in space with a single instrument in the energy range from ~ 80 MeV/n to ~ 3 GeV/n. Solar helium (up to 1 GeV/n) and protons (up to ~ 3 GeV/n) were recorded. A study on the comparison between PAMELA data and Neutron Monitors, GOES and Ice Top was carried out, together with a deep study on the spectral shape fitting. More details can be found in [12]. Since then PAMELA collected many data from other solar events, which are now under analysis.

Another great challenge in constraining scenarios for SEPs acceleration is due to the fact that the signatures of acceleration itself are heavily modified by transport within interplanetary space. During transport, SEPs are subject to pitch angle scattering by the turbulent magnetic field, adiabatic focusing, or reflecting magnetic structures. Ground Level Enhancements (GLEs), such as the 2012 May 17th one, provide an ideal way to study acceleration with minimal transport. PAMELA presented in [13] a unique high-energy SEP observation from the May event and interpreted the observed pitch angle distributions as a result of local scattering (1 AU) by the Earth's magnetosheath. For these studies new analysis method were developed to estimate SEP energy spectra as a function of the particle asymptotic pitch angle. The crucial ingredient is provided by an accurate simulation of the asymptotic exposition of the PAMELA apparatus, based on a realistic reconstruction of particle trajectories in the Earth's magnetosphere. The results of this backtracing procedure are shown in figure 8(a), where the

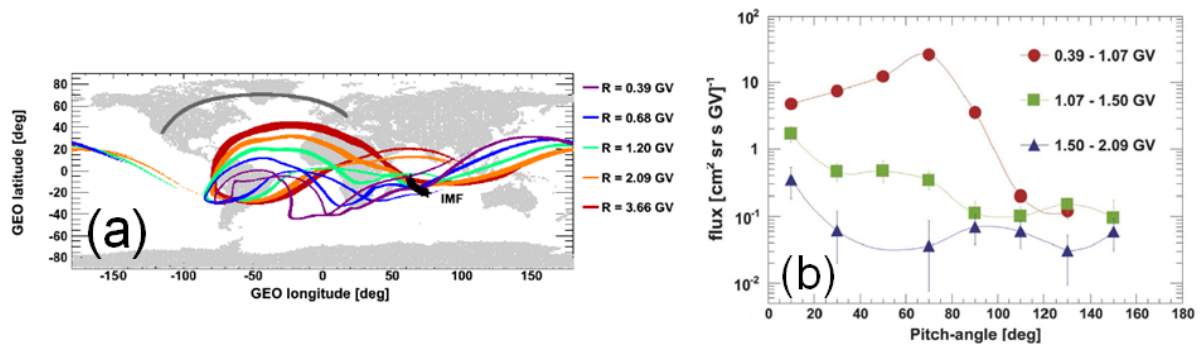


Figure 8. Asymptotic cones of acceptance of the PAMELA apparatus for sample rigidities for the first PAMELA polar pass (a). PAMELA's pitch angle distribution (background subtracted) in 3 rigidity ranges (b).

asymptotic cones of acceptance of the PAMELA apparatus for sample rigidities (evaluated in geographical coordinates) are depicted for the first PAMELA polar pass (0157-0220 UT) of May 17th.

Figure 8(b) shows PAMELA's pitch angle distribution (background subtracted) in 3 rigidity ranges. PAMELA observed two populations simultaneously with very different pitch angle distributions: a low-energy component (0.39-1.07 GV) confined to pitch angles $<90^\circ$ and a high-energy component (1.50-2.09 GV) that is beamed with pitch angles $<30^\circ$. Studies showed that this is the first observation of differential dispersion as particles transit the magnetosheath. More details can be found in [13].

10. Earth's magnetosphere: geomagnetically trapped and albedo particles

Data from the PAMELA were also used to perform a detailed measurement of under-cutoff protons at low Earth orbits. On the basis of a trajectory tracing approach using a realistic description of the magnetosphere, protons were classified into geomagnetically trapped and albedo. The former include stably-trapped protons in the South Atlantic Anomaly, which were analyzed in the framework of the adiabatic theory, investigating energy spectra, spatial and angular distributions. The albedo protons were classified into quasi-trapped, concentrating in the magnetic equatorial region, and un-trapped, spreading over all latitudes.

Previously, PAMELA has provided the first evidence of the existence of a stably-trapped antiproton population in the inner radiation belt [14], mostly generated by the decay of albedo antineutrons (CRANbarD, in analogy to trapped protons). The trapped proton results are depicted in figure 9(a), while the trapped antiprotons are visible in figure 9(b).

Precise measurements of electron and positron fluxes in energy range from 80 MeV to several GeV below the geomagnetic cutoff rigidity and trapped/albedo cosmic ray deuteron fluxes were also carried out using the PAMELA magnetic spectrometer. More details on the magnetospheric analysis can be found in [15, 16, 17, 18].

Conclusions

In this paper we tried to highlight some of the most important results of the instrument PAMELA, flying in orbit for ten years. Space limitations did not allow a complete and detailed picture of the huge amount of scientific data that the mission has provided, that can be found instead in the references.

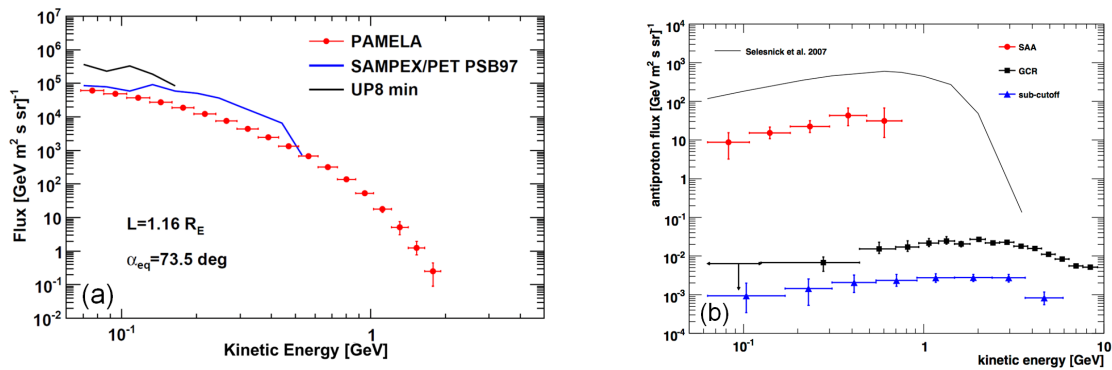


Figure 9. PAMELA trapped proton energy spectrum (a), and trapped antiproton spectrum (b) measured by PAMELA in the SAA

References

- [1] Adriani O *et al.* 2014 *Phys. Rep.* **544** 323
- [2] Adriani O *et al.* 2011 *Science* **332** 69
- [3] Adriani O *et al.* 2011 *Phys. Rev. Lett* **106** 201101
- [4] Adriani O *et al.* 2014 *Astr. J.* **791** 93
- [5] Mayorov A G *et al.* 2011 *JETP Lett.* **93** 628
- [6] Adriani O *et al.* 2015 *Phys. Rev. Lett.* **115** 111101
- [7] Adriani O *et al.* 2010 *Phys. Rev. Lett.* **105** 121101
- [8] Adriani O *et al.* 2009 *Nature* **458** 607
- [9] Adriani O *et al.* 2013 *Astr. J.* **765** 91
- [10] Adriani O *et al.* 2015 *Astr. J.* **810** 142
- [11] Adriani O *et al.* 2016 *Phys. Rev. Lett.* **116** 241105
- [12] Adriani O *et al.* 2011 *Astr. J.* **742** 102
- [13] Adriani O *et al.* 2015 *Astr. J. Lett.* **801** L3
- [14] Adriani O *et al.* 2011 *Astr. J.* **737** L29
- [15] Adriani O *et al.* 2015 *J. of Geo. Res.* **120** 3728
- [16] Adriani O *et al.* 2015 *Astr. J. Lett.* **799** L4
- [17] Adriani O *et al.* 2009 *J. of Geo. Res.* **114/A12** A12218
- [18] Koldobskiy S A *et al.* 2015 *JPCS* **632** 012060